

AD-A102 556 NAVAL RESEARCH LAB WASHINGTON DC
NUCLEAR RESONANCE PROFILING DATA ANALYSIS. (U)
AUG 81 K L DUNNING
UNCLASSIFIED NRL-NR-4332

F/6 20/8

NL

1 of 1
40 A
102-046

END
DATE
FILED
9-81
OTIC

ADA102556

REPORT DOCUMENTATION PAGE		READ INSTRUCTIONS BEFORE COMPLETING FORM
1. REPORT NUMBER	2. GOVT ACCESSION NO.	3. RECIPIENT'S CATALOG NUMBER
NRL Memorandum Report 4332	AD-A102 556	
4. TITLE (and Subtitle)	5. TYPE OF REPORT & PERIOD COVERED	
NUCLEAR RESONANCE PROFILING DATA ANALYSIS	Final report on this phase of this problem.	
7. AUTHOR(s)	6. PERFORMING ORG. REPORT NUMBER	
K. L. Dunning	16) RR 04202	
9. PERFORMING ORGANIZATION NAME AND ADDRESS	10. PROGRAM ELEMENT, PROJECT, TASK AREA & WORK UNIT NUMBERS	
Naval Research Laboratory Washington, DC 20375	11) 61153N; RR 04202-418 66-0446-0-1	
11. CONTROLLING OFFICE NAME AND ADDRESS	12. REPORT DATE	
12) 14) NRL-MR-4332	13) August 11, 1981 (11) 11	
14. MONITORING AGENCY NAME & ADDRESS (if different from Controlling Office)	15. SECURITY CLASS. (of this report)	
14) NRL-MR-4332	UNCLASSIFIED	
16. DISTRIBUTION STATEMENT (of this Report)	15a. DECLASSIFICATION/DOWNGRADING SCHEDULE	
Approved for public release; distribution unlimited.		
17. DISTRIBUTION STATEMENT (of the abstract entered in Block 20, if different from Report)		
18. SUPPLEMENTARY NOTES		
19. KEY WORDS (Continue on reverse side if necessary and identify by block number)		
Materials analysis	Solid-state devices	
Nuclear resonance profiling	Computational methods	
Van de Graaff accelerator		
20. ABSTRACT (Continue on reverse side if necessary and identify by block number)		
Analysis methods are described which were developed at NRL over the past decade and used to treat data obtained from nuclear resonance profiling measurements made at the NRL 5-MV Van de Graaff Accelerator. Principles are discussed which are the basis for making measurements and, from results, determining the absolute concentration as a function of depth (below a well-defined surface) of an element which may be the sole constituent of a solid or a very small fraction thereof. Procedures are described for		
(Continues)		

DD FORM 1 JAN 73 1473

EDITION OF 1 NOV 68 IS OBSOLETE
S/N 0102-014-6601

SECURITY CLASSIFICATION OF THIS PAGE (If Any) **UNCLASSIFIED**

(Continues)

252950

sel

20. ABSTRACT (Continued)

obtaining pertinent Fortran source-language files, object-language files, load modules, and job-specification-language files from the catalog of the NRL Texas Instruments ASC7 computer. Instructions for the use of these programs and remarks supplementing instructional annotation in the source-language versions are recorded. Concluding remarks are made which bear on future software design, computers and peripheral apparatus, and computer languages suitable to the development of facilities related to nuclear resonance profiling and similar endeavors.

CONTENTS

I. INTRODUCTION	1
II. PRINCIPLES OF NUCLEAR RESONANCE PROFILING	3
A. General Features of an Example	3
B. Beam-Energy Distributions	3
C. Gamma-ray Yield Functions	5
III. PROFILE DETERMINATION	7
IV. EXISTING SOFTWARE	10
A. Initial Data Treatment	10
B. Matrix Computation	11
C. Yield Computation	14
V. CONVERSION OF RELATIVE PROFILES TO ABSOLUTE PROFILES	16
A. Thin Targets	16
B. Thick Targets	16
VI. CONCLUDING REMARKS	17
A. Software Architecture	17
B. Computers and Peripheral Apparatus	18
C. Computer Languages	18
VII. ACKNOWLEDGMENTS	20
REFERENCES	21
APPENDIX	22

NUCLEAR RESONANCE PROFILING DATA ANALYSIS

I. INTRODUCTION

The purpose of this report is to describe some of the methods developed at NRL during the past decade for nuclear resonance profiling (NRP) with the principal objective of providing aid to those at NRL who wish to use these methods for the acquisition and analysis of pertinent data.

In this report, NRP will mean the acquisition and analysis of nuclear reaction data obtained with incident ion energies in the neighborhood of a narrow nuclear resonance for the purpose of measuring the absolute concentration of some element as a function of depth in the near-surface region of a solid. The term near-surface is meant to designate a region a micrometer or less below a well-defined surface of a solid with cross-sectional area the size of the incident ion beam. Concentration as a function of depth will be referred to as a concentration function or a profile.

The methods described herein are rooted in the development at NRL of a versatile Van de Graaff accelerator with a set of sophisticated ancillary apparatus, research in nuclear physics (especially in connection with sharp (p, γ) resonances), and the need for precise "impurity profiles" in the near-surface region of materials useful in the development and fabrication of solid-state electronic devices. Emphasis in this development was given to situations where existing methods of measurement were inadequate.

When the use of NRP methods is contemplated, a large collection of methods based upon the bombardment of a specimen with particles or electromagnetic radiation and the consequent emission of particles and/or radiation should be considered. An impressive array of such methods has been developed within the past decade and most of these are more convenient, more rapid, and less expensive than NRP. However, there are problems in material analysis where NRP can yield results not obtainable by other means. For example, much of the impetus for NRP at NRL came from the need for sodium impurity profiles in SiO_2 about 1972. It was found that sodium distributions changed when measurements were attempted by means of secondary-ion mass spectroscopy (SIMS) but not during NRP measurements (1).

Detection limit is an important parameter in materials analysis and is here taken to mean the minimum concentration (of the element of interest in the test specimen) for which useful information can be obtained. A particular detection limit must be associated with a particular set of measurement parameters. When profiles fall below "zero" in discussions and diagrams which follow, the implication is that the particle emission or radiation upon which the measurement is based is not detectable above background effects (which are subtracted before analysis). That is, the concentration of the element of interest is below the detection limit for the method used.

Although it is possible to measure absolute concentrations by making use of known reaction cross sections, detector efficiencies, and geometric factors, measurements can be more accurately and conveniently made by first obtaining a depth profile of relative concentration and then making a second measurement (with only the target changed) on a specimen with a known

number of target atoms (of the element of interest) all in the near-surface region.

The raw data obtained in NRP measurements is in the form of a set of particle or photon counts expressed as a function of incident ion energy. This function is an approximate profile (especially for narrow resonances) and is frequently adequate for many uses (when converted to concentration as a function of depth). However, one of the purposes of the work upon which this report is based was to establish depth-concentration profiles that are nearly independent of background effects, ion-beam-energy distributions, ion energy-loss straggling and resonance widths.

Following this introductory section, there will be a discussion of the principles of NRP, the methods of computation, a discussion of existing software, the conversion of relative to absolute concentration profiles, and concluding remarks with suggestions for future development.

II. PRINCIPLES OF NRP

This discussion of the principles of NRP will be aided by an illustrative example, a measurement (made in January 1979) of hydrogen concentration in an SiO_2 -Si specimen (target) by means of the reaction ${}^7\text{Li}(\text{H},\gamma){}^8\text{Be}$. The atoms of the element that participates in the reaction upon which the measurement is based will be called the target atoms. The method described need not be confined to (p,γ) reactions; (p,α) reactions have also been used.

A. General Features of the Example. Figure 1 shows the relative gamma-ray yield (counts per minute in a specified energy window) from the ${}^7\text{Li}(\text{H},\gamma){}^8\text{Be}$ reaction (circles and left linear vertical scale) and the absolute hydrogen concentration (solid histogram) as functions of the ${}^7\text{Li}^+$ incident energy relative to the resonance energy (3,050 keV) for the target sketched in the upper part of the diagram. Note that the concentration scale and profile are truncated at the lower end.

The angstrom depth scales are fixed by taking the ion-energy (above resonance) to be numerically equal to the energy loss (in keV) at the depths indicated. The specific loss rates (stopping powers) are those of Si and SiO_2 (presence of H ignored) and, therefore, the angstrom depth scale factors for SiO_2 and Si are different. The specific energy loss rates are considered to be constants for the depths spanned. The thickness (depth) of the SiO_2 layer was known from sample fabrication methods but, in principle, could have been measured by methods described in this report.

The difference in shape between the profile and the gamma-ray yield curve is due to the vacuum beam-energy distribution (VBED), the cross-section shape and the beam-energy-loss straggling. By careful analysis, the true profile can be determined from the gamma-ray yield curves to an approximation dependent upon the statistical merits of the data.

B. Beam-Energy Distributions. The VBED was determined in the measurement of the example by a magnetic beam analyzer followed by an electrostatic beam analyzer (EBA). The theoretical VBED is triangular in shape but (partly because of slit-edge scattering) can be well represented by a Gaussian with its mean energy equal to the Van de Graaff terminal voltage (singly charged ions) and its full width at half maximum (FWHM) determined by the EBA aperture settings (2). In the example, the VBED is represented by a Gaussian with a FWHM of 1.5 keV. In later parts of the report, the VBED will be represented by $g(E_{\text{in}}, E_b)$ where E_b is the mean energy and $g dE_{\text{in}}$ is the probability that a beam particle will be in energy interval dE_{in} at E_{in} . The method of analysis will hold, of course, for a VBED of any shape. For convenience, the VBED may be normed to unit area. That is, the probability that a projectile will be in some energy interval of the representation is unity.

As the beam ions enter the target, they lose most of their electrons; the average energy is degraded (at pertinent average energy loss rates); the distributions are broadened (increasingly with depth) and skewed by statistical fluctuations in energy loss (straggling).

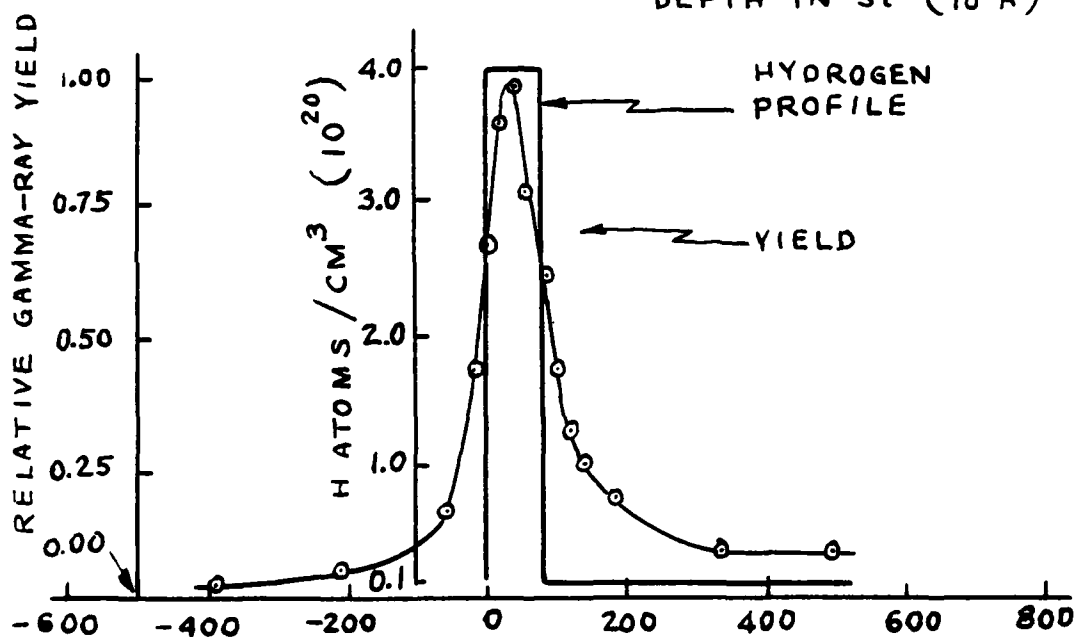
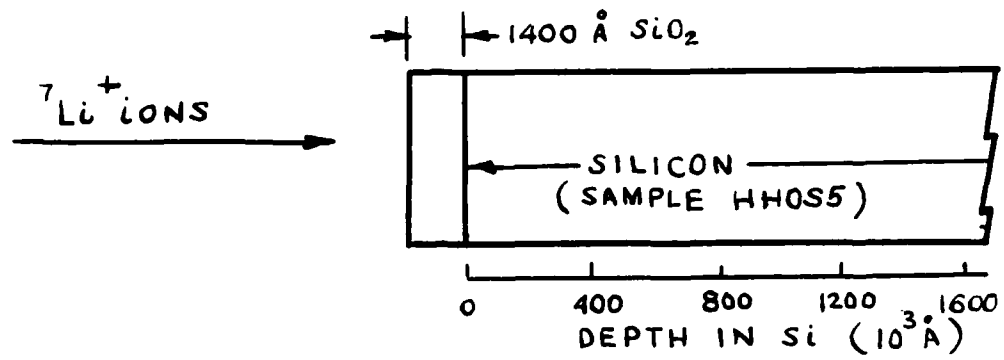


Fig. 1 - Relative gamma-ray yield (circles) and H-atom concentration (solid line) for sketched target

We may represent the internal beam-particle energy distribution (IPED) at depth x within the target by $h(E_b, E, x)$, $h dE$ being the probability that a particle will be in energy interval dE at E . An IPED is broader than the VBED and has a mean energy which is lower by the average energy loss of the projectiles over the paths to depth x . The function $h(E_b, E, x)$ can be calculated with the help of a straggling function $f(E, E_{in}, x)$ where $f dE$ is the probability that a particle in energy interval dE_{in} at E_{in} before entering the target will be degraded into energy interval dE at E as it is slowed (mostly by electronic stopping) enroute to depth x . We then have

$$h(E_b, E, x) = \int_{E_{in}} g(E_b, E_{in}) f(E, E_{in}, x) dE_{in} \quad (1)$$

where the integral extends over the VBED.

C. Gamma-ray Yield Functions. If the incident ion energy is increased in suitable steps from below resonance energy to well above resonance energy, and a photon counter (with an appropriate energy window) intercepts a constant fraction of the emitted gamma rays, a relative gamma-ray yield function such as that plotted (circles) in Fig. 1 will be obtained. The NRP method is most effective when there is a strong, narrow, isolated resonance for capture of the incident atoms into a compound nucleus. A narrow resonance provides good similarity between the profile and the yield shape at shallow target depths where straggling is small and provides for better ultimate depth resolution than does a broad resonance. It is assumed for this discussion that there are no resonances associated with the host materials in the incident energy region of interest. If there are, the associated yield (as well as any nonresonant yield from the host and target atoms) must be subtracted before further data analysis.

The absolute gamma-ray yield function for an "impurity" element in a homogeneous host of thickness, T_x , can be represented by

$$Y_{abs}(E_b, T_x) = N_{in} \epsilon \int_{E=0}^{T_x} N_T \phi(x) h(E_b, E, x) \sigma(E_r, E) dE dx \quad (2)$$

Where ϵ is the efficiency and solid-angle factor of the detector; N_{in} is the number of incident ions; $N_T \phi(x)$ is the concentration (atoms/cm³) function for the element being profiled; $h(E_b, E, x)$ is the IPED; N_T is the total number of atoms/cm² to depth T ; $\sigma(E_r, E)$ is the cross-section function. Since only the relative yield is of interest in the description ahead, the subscript abs and the factors N_{in} and ϵ may be dropped. The functions under the integral signs may be normed as convenience dictates. Absolute profiles are derived from relative profiles by means of data from a calibration target of known composition; this will be discussed in Section V. Although targets may be composed of several homogeneous layers of different materials, the analysis must deal with each homogeneous layer separately because of its particular specific average energy loss rate. Note that yield is a function of target thickness T_x . For a target of moderate thickness, this dependence is negligible (for a narrow resonance) except near the end of the target.

The integrand of equation (2) can be viewed as a product of three probability factors (all normed to unit area for this paragraph). $N_p\phi(x)$ is the probability that there is one atom per unit area in target element dx at depth x ; $h(E_b, E, x)$ is the probability that for incident energy E_b there will be a projectile at depth x with energy E ; $\sigma(E_r, E)dE$ is the probability for gamma-ray emission due to the element dE at E of the cross-section function if there is one target atom per unit area in element dx at x .

In the analysis of NRP data, it is convenient to express target depth in terms of $\bar{\Delta}(x)$, the average energy loss of a projectile in penetrating to depth x , rather than in terms of angstroms or cm. If, in diagrams such as that of Fig. 1, the incident energy $E_b = E$ is associated with zero depth in the target, and the incident energy is increased from E_b to $E_b + \bar{\Delta}$, the average energy of the IPED at depth x will be E_r . The bombarding energy (relative to resonance energy) is numerically equal to the target depth in energy-loss units.

Equation (3) is an expression for relative yield with the depth variable in energy-loss units.

$$Y(E_b, T) = \int_{E_{in}} \int_E \int_0^T N(\bar{\Delta}) g(E_{in}, E_b) F(E_{in}, E, \bar{\Delta}) \sigma(E_r, E) dE dE_{in} d\bar{\Delta} \quad (3)$$

The order of integration is, of course, immaterial but it is often helpful to integrate with respect to dE_{in} first to give the analog of equation (2).

To recapitulate then, we see that, in order to calculate the relative gamma-ray yield function $Y(E_b, T)$, we need a concentration function $N(\bar{\Delta})$, a VBED, $g(E_{in}, E_b)$, a straggling function $F(E_{in}, E, \bar{\Delta})$, and a cross-section function $\sigma(E_r, E)$. In the example, a set of straggling functions (for a discrete set of $\bar{\Delta}$) is calculated from the theory of Vavilov (3). They could have been calculated from other theories and (for economy of computation time) should be calculated at different depths in the target by different methods; for example, by Vavilov's theory for shallow depths (for low-Z targets and projectiles only) and by Bohr theory (4) for greater depths. While the correspondence between yield and profile is most obvious for narrow, isolated resonances, there is no reason why the cross-section function cannot span more than one resonance. The detector energy window must be such that as the set of E_b is traversed, there is no yield from resonances other than those represented by the cross-section function. Recall also that any yield from the host must be considered as background.

III. PROFILE DETERMINATION.

The relative gamma-ray yield can be measured and can be calculated from equation (3) if the profile $N(\bar{J})$ is known. However, the objective is to measure function $Y(E_b, T)$ and from this measurement determine $N(\bar{J})$. This may be done by guessing at a profile after inspecting the measured yield function, calculating $Y(E_b, T)$, comparing measured and calculated yields, then adjusting $N(\bar{J})$ and iterating until the calculated and measured yield functions are judged to be in reasonable agreement. Machine calculations and plotting facilitate this method. For profiles of the shape of that of Fig. 1, good agreement can be obtained in about three trials.

To carry out numerical analyses, the entire target will be divided into elemental slices perpendicular to the depth axis. These slices will be labelled with index i ($i = 1, 2, 3, \dots$) with the surface slice labelled with $i = 1$. The slice widths, w_i , need not be uniform. This target subdivision will be independent of any subdivision into homogeneous layers of different stopping power (layered targets). Let us first consider the target to be homogeneous and later consider steps needed to treat layered targets.

In applications of the NRP method, the need frequently arises to determine the profiles of an "impurity" element in many identical hosts. For example, in solid-state device development, it may be useful to know the hydrogen profiles in the sample configuration of Fig. 1 for many identically prepared samples which have been subjected to a varied set of processing environments (annealing etc.). For this reason and as a basis for the possible development of a more sophisticated analysis method, it is useful to construct from equation (3) a matrix, M , characteristic of the reaction parameters, the mode of target subdivision, but independent of the profile. This matrix together with a vector, P , characteristic of the profile and the mode of target subdivision will permit calculation of the yield function according to

$$Y(E_b, T) = MP \quad (4)$$

where $Y(E_b, T)$ is a set of ordinates of the calculated yield function at a set of abscissas, $E_b - E_r$, the latter set being numerically equal to an energy-loss set corresponding to various depths into the target.

This suggests a method of profile determination without the need for iteration. If M can be inverted to M^{-1} , then

$$P = M^{-1}Y. \quad (5)$$

Some exploratory work has been done toward this goal but an algorithm for the inversion which will produce nonsingular inverse matrices with acceptable errors has not yet been devised.

The i th column of the matrix, M , is obtained by numerically integrating equation (3) with respect to dE_{in} and dE . The row indices, m , are those of the set E_b . The column indices, i , are those of the slices. The i th element of P is $N(\bar{J})w_i$. The yield associated with $(E_b)_m$ is then

$$Y_m = \sum_i M_{m,i} P_i \quad (6)$$

For targets composed of more than one homogeneous layer, (five is the maximum in the present software) the yield for a particular value of $(E_b)_m$ is obtained by summing the calculated yields for each layer, computed separately with the IPED for the first interface substituted for $g(E_b, E_{in})$ to get the contribution for the second layer and so on. That is, the projectile energy distribution to be used for obtaining the yield from the n th layer ($n = 2, 3, \dots$) is the IPED at its most shallow boundary.

The target subdivision scheme should be such that the number of subdivisions is kept to a minimum with the proviso that a finer subdivision will not alter the calculated yield function significantly. In some cases, it may be useful to choose the width of the first slice to be as small as ten angstroms if the incident energy distribution and the resonance are very narrow and precise information very near the surface of the target is wanted. The slice widths, w_i , may increase approximately as the square root of the depth (without losing obtainable details of the calculated yield function) since straggling effects increase in this manner and they tend to smear sharp details in the parts of the measured yield curve associated with the interior slices of the target.

Once the target subdivision scheme has been chosen, a set of functions $F_i(\Delta, \bar{\Delta}_i)$ must be calculated, one for each slice; Δ is the exact energy loss of a projectile enroute from the surface of a target layer to the center of the i th slice; $\bar{\Delta}_i$ is the average energy loss in keV from the layer surface to the center of the i th slice. The present software calculates the set F_i by means of Vavilov's theory (3) which has limited applicability as will be discussed later.

In our example, $g(E_b, E_{in})$ is represented by a Gaussian function and $\sigma(E, E_r)$ by a Breit-Wigner single-resonance function.

Many NRP calculations and plots have been made with the NRL Texas Instruments Advanced Scientific Computer (ASC7) via a keyboard terminal. Data and program files associated with the illustrative example are in the ASC7 catalog at node USERCAT/D66/B00/DUNNKL/NRP* which will be replaced with the JSL** synonym, P5, in the following discussion. The source language is Fortran.

Some detail concerning the software will appear in the next section but what follows immediately will simply show how to use files and programs pertinent to the example.

* The symbol \emptyset represents zero.

** ASC7 job specification language.

The files needed to run the calculation of the example are sons of the catalog node P5; that is, e.g., P5/SL9YMAT is the catalog path to the source-language file of the program YMAT that calculates the matrix. The object-language file and the load module for YMAT are the sons OL9YMAT and LM9YMAT respectively. The input data file (son) is IN2TGT7 and the output file containing the matrix is MA2TGT7. Usually the scheme has been to label NRP files with the first two characters indicating the kind of file, with the next character as a "serial number" indicating a particular version, and with the last four characters indicating that the file is associated with a particular program or target.

The computer run of the program YMAT may be made with the help of the file at P5/HLP7, suitably modified. This is a JSL file and may be run from a keyboard terminal, piecewise if desired. There is provision for a file named FT59F001 which contains diagnostic plots which may have been initiated in the input file, IN2TGT7, at the user's option.

Before making use of the matrix of our example, let us turn to the processing of the experimental data and the cataloging of the results in a form that will be suitable for comparison with calculated yield. The results of measurements have been formatted and filed at P5/OXHHOS5. A JSL program similar to that at P5/HLP5 facilitates the processing of experimental data via program DATA5 with source-language, object-language, and load-module files at P5/S11DATA5, P5/OL1DATA5, and P5/LM1DATA5 respectively. Program DATA5 provides for a plot of the experimental data that will be needed for the later conversion of a relative profile to an absolute profile. The output file of DATA5 is catalogued at P5/OX1HHOS5.

The next step is to prepare a file containing a trial profile, merge it with the experimental data file, OX1HHOS5, and with the file MA2TGT7. This merged file for the example is at P5/IMHHOS5.

This merged file is the input file for program YMULT that performs the matrix multiplication and produces a plot of the essential information of Fig. 1. The source, object, and load-module files for YMULT are at P5/SL8YMULT, P5/OL8YMULT, and P5/LM8YMULT respectively. The JSL list at P5/HLP3 or one similar to it can be of help in running YMULT.

If the plotted calculated yield does not compare favorably with the plotted measured yield, the profile of file IMHHOS5 can be altered and another YMULT run made.

IV. EXISTING SOFTWARE.

Fortran programs for carrying out the kind of analysis described in preceding sections of this report reside in the catalog of the NRL Texas Instruments ASC7 computer. Program listings will not be given. Instead, catalog path names to pertinent files will be given and programs will be discussed with the help of the example of Fig. 1.

The source-language programs are annotated so that, hopefully, they can be understood and used with a reasonable effort. These programs were written with small effort toward sophistication but rather with the goal of creating and using the software in applications of some urgency. Therefore, they are not in the exceedingly rare category of programs that cannot be modified to better serve the user.

The catalog path names for files pertinent to this report will include the JSL synonym, P5 = USERCAT/D66/B00/DUNNKL/NRP. A catalog status print-out for the node associated with this path appears in the Appendix. The JSL listings at P5/HPL1, P5/HLP3, etc. may be of some help in running and in modifying the programs.

A. Initial Data Treatment. The data obtained from measurements is entered into a file to be read by program DATA5. The names of the quantities, their meanings, and formats can be obtained from the source-language listing at P5/S11DATA5 and the input file for the example at P5/IXHHOS5.

Program DATA5 first reads and prints the input file which (for purposes of this discussion) will be said to consist of card images named: 1,2,3,4a,4b,****, and 5. On the first run, set NBRREJ = \emptyset in image 1 and omit image 2. If the results of the first run show that there are N obviously wild data points among those represented in images 4a, 4b, ***, set NBRREJ = N; enter the ordinal numbers of the points to be rejected in image 2 and make a second run with the amended file. If NBRREJ $\neq \emptyset$, subroutine CHANGE will be called to make the deletion. Experience indicates that this feature of the program is almost never used.

Card image 3 (second image in file IXHHOS5) may contain up to 50 Hollerith comment characters. In the input file for the example, "NO TILT" means that the beam was striking the target 90 degrees to the plane of the target; (some smaller angle could be used to enhance depth resolution). The notation "NWCT = 79.0" indicates that the controlled temperature of the EBA (northwest corner temperature) was 79.0 degrees Fahrenheit.

Card image 4a contains data for the first three measurement points, the data for each point consisting of an ordinal number (NRUN), the time of the run in minutes, the number of yield counts, and the potentiometer setting (of the EBA). These data are entered in order of increasing potentiometer (beam energy) settings. Card image 5 contains six numbers. The first is the potentiometer constant (POTCST * POTSET * 1000 gives the beam energy in keV).

BG1CST is the number of counts per minute obtained in a background run with the beam hitting a stopper (distant from the target). SDBG1 is calculated by the user according to the formula $\text{SQRT}(\text{BG1CST}/(\text{number of minutes for background run}))$. This quantity is the standard deviation of BG1CST.

The third number in card image 5 permits the average yield for the first NEG2 points to be subtracted from all points; NEG2 = \emptyset means no subtraction. This constant facilitates the subtraction of a pre-resonance beam-dependent background under the following circumstances. If a single, narrow, isolated resonance is the basis for the measurement and the bombarding energy for the first point is far below the resonance energy, the yield for the first few points will be essentially that due to the host and the tails of any distant resonances; this background should be subtracted from all points. For example, if the yield from the first three data points is small and nearly equal, set NEG2 = 3. No subtraction of this kind was made for the analysis of the example.

The last three numbers in card image 5 have meanings as follows. NPLOT = 1, (\emptyset) causes (prevents) the calling of subroutine GRAPH3 which creates a plot file (FT59F \emptyset /1) which can be used to actuate a Calcomp plotter to produce a plot of the experimental data. This plot will show the raw yield counts (squares), the yield after time-dependent background subtraction (crosses), the yield after target-dependent background subtraction (triangles), and vertical lines indicating the standard deviation. NPNCH = 1, (\emptyset) causes (prevents) the punching of the output file onto cards (file OX1HHOS5 for the example). NFILE = 1, (\emptyset) causes (prevents) the printing of the output file when DATA5 is being run.

The plot of experimental data is useful (as will be explained in Section V) for converting relative concentration profiles to absolute concentration profiles.

A more accurate method of determining the beam-dependent background consists of obtaining a measured yield curve for the host devoid of the impurity (element of interest) for an identical set of bombarding energies and making a point-by-point subtraction to provide input data for program DATA5. This is especially feasible when the impurity is an implanted one.

B. Matrix Computation. The matrix, M, of equation (4) is computed by program YMAT with source-language file at P5/SL9YMAT, object file at P5/OL9YMAT, and load module at P5/LM9YMAT. This matrix is dependent upon beam parameters, resonance parameters, and all target parameters except the concentration function (profile) of the element of interest. It is obtained by integrating equation (3) with respect to E and Ein. The integration with respect to $\bar{\Delta}$ is replaced by matrix multiplication carried out by another program named YMULT.

The YMAT source-language listing contains many comments and a card-image table for the input file. A convenient way to create a new input file for YMAT is to display an existing input file (for example, that for our illustrative example at P5/IN2TGT7) on a keyboard terminal and alter it as needed.

The source-language listing may be used to obtain an understanding of program YMAT. Additional comments which will be of help follow.

The statement labels in the Fortran listing are not always in ascending order; this is due in part to the use of blocks of statements from earlier programs.

Program YMAT first reads and prints the input file (IN2TGT7 for our example).

The next action is to compute the parameters needed for the division of the target into slices; later, an energy-loss distribution function (ELD) will be associated with each slice. The average loss for a particular ELD will be that to the center of the associated slice. The slices at the surface of the target will have thicknesses a few times the FWHM of the VBED. The interior slices will increase in thickness with depth into the target at a rate roughly proportional to the increase in energy-loss straggling with depth in order to minimize the number of slices without sacrificing depth resolution. That is, the interior resolution is limited by the FWHM of the IPED which increases with depth due to straggling. The widths of the ELD increase roughly as the square root of depth of penetration. This subdivision into slices spans the various homogeneous layers that may exist.

After reading and printing the input file, program YMAT calls subroutine LAMGR (layer manager) to select the current (initially the first) homogeneous layer.

The next task is to compute parameters needed in the calculation of the ELD set. The calculation of these functions is based upon a theory due to P. V. Vavilov (3) and a modification of a program kindly supplied by S. M. Seltzer and M. J. Berger (5). A discussion of the suitability of this theory for the purpose at hand will be found in the final section of this report. The loss axis for the ELD set must span a domain great enough to accommodate the greatest loss suffered in the target by any beam particle; in application, this means that the loss domain must extend from zero to some value somewhat greater than the target thickness. For purposes of ELD calculation, the loss axis is divided into uniform intervals of width DE with ordinal numbers, K, (sometimes J5); the interval of greatest loss is designated by K = 1; the ordinal numbers increase with decreasing loss.

To save computer costs, the ordinates of the ELD are not calculated in detail for every loss interval, DE, except in the low-loss region. Rather, the loss axis is divided into blocks and the ordinates for some intervals are supplied by interpolation as explained in the Fortran listing. A maximum of five blocks is provided for; the detailed calculations are less dense as the block numbers increase.

The independent variable in the Vavilov functions is not energy loss but is a quantity named lambda which is a function of the exact energy loss and the average energy loss of interest. These functions must be converted into functions of actual energy loss before use in this analysis.

In the midst of the ELD parameter calculations, the target slice widths are calculated by calling subroutine TARG1 which may, in turn, call TARG2 and TARG3. Upon completion of these tasks, many of the quantities calculated up to this point by the main program (YMAT) are printed.

A set of bombarding energies, EB(M), is needed for the calculation of the matrix elements; the rows of the matrix, M, are labelled by the integer variable, M; this set need not intersect the set of bombarding energies used in the measurement. The YMAT input file contains parameters which permit the set EB(M) to have intervals of three different sizes in order to accommodate the sharp rise in yield at the target surface associated with narrow resonances. The set of bombarding energies, the resonance function, and the VBED are calculated by calling subroutine SETS6.

Subroutine SETS6 calculates a Gaussian VBED using the FWHM provided in the input file. This function is arbitrarily cut off at 1.5 FWHM since the exact shape of the VBED is not known (theoretically, it is a triangle modified by slit-edge scattering)(2). The cross-section function is calculated by means of the Breit-Wigner single-resonance formula with the skirts cut off when the magnitude of the abscissa is NGAM FWHM, where NGAM is from the input file. The density of ordinates calculated is decreased in the regions remote from the peak of the resonance function to save computation time. To encompass all but a few tenths percent of the area under the curve, the abscissas must be extended to about 100 FWHM on either side of the peak. In the present calculations, cutoff can be made much sooner without significant effect.

The beam energy distribution and the resonance function can be plotted for diagnostic purposes at the option of the user. Subroutine GRAPHC is called for this purpose if parameters are set in the input file as explained in the listing.

Program YMAT is now ready to calculate (by columns) the elements of the matrix M. The column index is I (which also designates a target slice and the ELD associated with that slice). The calculation begins with the lowest I-value for the current homogeneous target layer and with the ELD of greatest width (smallest K).

Subroutine VAV7 is called to compute the ELD for the Ith slice and, in turn, calls subroutine TRIGEX to supply certain needed functions. Parameters in the input file (see card-image table in the listing) permit considerable diagnostic printout. Provision may be made (in the input file) to plot (via subroutine GRAPH6) selected ELD in order to see if they have reasonable shapes, smoothness, and cutoff.

Next, subroutine IPED2 is called to provide an IPED shape for the current target layer. This is the VBED shape for the surface layer; for interior layers, this shape must be modified to take into account the average energy loss and straggling in earlier layers. This shape is then used in conjunction with the set of bombarding energies, EB(M) to provide IPED for the integration with respect to E in equation(2). Note that the IPED corresponds to the $h(E_b, E, x)$ of equation (1).

Subroutine YINT is called to perform the integration over E of equation (3) to produce the matrix element for current M and I. After this is done for all M (all elements in the Ith column), I is advanced and the submatrix for the current layer is completed.

The submatrices for other target layers are computed and the yield for a uniform (unit height) concentration function is computed for diagnostic purposes and may be plotted at the option of the user.

The YMAT output file, which contains the matrix and other information for transmission to program YMULT, is written to a file and cataloged. That of our example is at P5/MA2TGT7.

This program may be run on the ASC7 with a JSL listing similar to that at P5/HLP7.

C. Yield Computation. The program YMULT computes the yield function by multiplying a trial profile function by the matrix, M, which was generated by program YMAT.

The YMULT input file for the illustrative example is cataloged at P5/IMHHOS5. The first two card images contain constants that control the reading, printing, and plotting done by YMULT. These are followed by three merged files; the first is the output file from DATA5 which, for our example, is cataloged at P5/OX1HHOS5. The next is a trial profile which, for convenience, has a maximum value of unity. The normalization can be chosen at will because we are calculating a relative profile. Next is the output file of the program YMAT which, for our example, is cataloged at P5/MA2TGT7. This YMULT input file can be conveniently formed by modifying an existing file and merging files at a keyboard terminal.

Program YMULT can be run on the ASC7 with a JSL listing similar to that cataloged at P5/HLP5. The source-language listing, object listing, and load module are at P5/SL8YMULT, P5/OL8YMULT respectively.

The following remarks together with the Fortran listing will be of help in understanding and in the use of program YMULT.

There is provision in YMULT to read and process more than one trial profile function but this feature has been seldom used.

The actual matrix multiplication is accomplished by calling subroutine MULT. The rows of the matrix computed by YMAT are multiplied into a column vector with each element composed of the product of a concentration value associated with the Ith target slice and the width (in energy-loss units) of the Ith slice in order to produce a yield value for each bombarding energy, EB(M). This is done for each target layer and the layer yields summed in an appropriate manner.

At the option of the user, YMULT will call subroutine GRAPHD to create a file for the Calcomp plotter, thus providing for plots of the kind shown in Fig. 1 - except that, in addition to the profile (which will be plotted with + signs) and measured gamma-ray yield (which will be plotted with octagons), the calculated yield will be plotted (with triangle symbols).

If inspection of this plot shows that the agreement between the measured and calculated yield is satisfactory in the user's judgement, the trial profile plotted can be considered a useful approximation to the actual profile. If not, the trial profile may be altered and another run of YMULT made.

To facilitate comparisons of the measured and calculated yields, the experimental yield is scaled for plotting so that the areas under both curves out to an abscissa EBNRM (a parameter inserted by the user into the YMULT input file) are equal.

All plotting programs described in this report were written for the CDC 3800 computer and, therefore, in the linking run (see JSL listing catalogued at P5/HLP4) the module at USERCAT/LIB/SUP/OBJECT must be assigned to the job to permit the ASC7 to use the CDC 3800 code.

V. CONVERSION OF RELATIVE PROFILES TO ABSOLUTE PROFILES.

Relative NRP concentration profiles may be converted to absolute concentration profiles by means of the absolute interaction cross-section function, geometric factors, detector efficiency, and other parameters associated with a measurement. This may also be done with the help of measured yield functions from calibration targets of known target-atom concentrations. The latter method is probably more convenient and accurate than the former and will be discussed for thin and thick targets.

A. Thin Targets. Targets that produce yield curves that (for narrow resonances) rise from zero yield (with background subtracted) at low bombarding energies and fall to zero again at higher (attainable) bombarding energies will be termed thin targets. A yield function associated with a thin target will be referred to as an entire function. Consideration of equation (2) shows that the area under a yield curve that is an entire function is proportional to the total number of target atoms/cm², N_T . The constant of proportionality may be found from the area under a measured yield curve for a thin calibration target with a different but known N_T . An example of such a calibration target is a metal or semiconductor host implanted with a known number of target atoms/cm², all in the first few thousand angstroms below a well defined surface. Convenient units for such constants are

$$\frac{(\text{No. of target atoms})/\text{cm}^2}{(\text{keV counts})/\text{microcoulomb}} .$$

The area under the relative profile must be equal to N_T for an unknown thin target. This allows a scale (atoms/cm³) to be placed upon the relative profile showing the absolute concentration for the unknown target as a function of depth.

B. Thick Targets. The yield for a thick target is not an entire function of the bombarding energy and the analysis for thin targets does not pertain. That is, the yield does not fall to zero near the end of the attainable bombarding energy span. Procedures for establishing concentration scales by means of thick calibration targets based upon careful considerations (not recorded here) follow.

The measured yield curve for a thick calibration target of known uniform target-atom concentration will, after an initial rise from zero (narrow resonance assumed), achieve a constant value and remain there for the remainder of the bombarding energy span. Some selected area entirely under the constant part of the curve (keV counts) can be used to determine a constant which may be used with thin targets of unknown concentration as previously described, provided that the (No. of target atoms)/cm² is that associated with the segment of the target spanned by the selected area.

If the target of unknown concentration is thick, a convenient value of T must be selected; the associated calculated yield curve must have this value of T ; the measured yield curve must be converted to an entire function by means of T and the calculated yield curve associated with the relative profile. The concentration scale may then be determined as before.

VI. CONCLUDING REMARKS.

This section contains a few general comments concerning nuclear resonance profiling computational methods which may be useful in possible future developments.

A. Software Architecture. As stated previously, the existing software was written with the object of producing working programs for urgent applications and without great concern for the user's convenience or computational costs. As the programs were used, it became evident that there is much room for improvement - especially with respect to the transparency and ease of application for the user. Computational costs can be reduced by restructuring software. Attention should be given to creating modules that can be run conveniently on computers smaller than the ASC7.

One fertile area for improvement concerns the computation of energy-loss distribution functions (ELD). Presently, a slight change in target configuration requires essentially the same set to be recomputed. In addition, all ELD are now computed from Vavilov's theory and interpolation methods were introduced to keep computation times within reasonable limits.

A great improvement could be made by computing sets of ELD and cataloging them in computer files in a form suitable for use by a program like YMAT. Only a few files of this kind would be necessary for measurements made in connection with solid-state device development, where only a few host elements and compounds are of interest such as Si and SiO₂ for example. These files might also be useful for other work involving energy-loss straggling.

Various computational methods could be used in creating a particular set. Considerable care and time could be spent on a set that is to be used many times. These sets could be used for other purposes such as, for example, in particle scattering analysis. As new theories and improved data appear, improved sets could replace existing sets without need to modify using programs.

Vavilov's theory agrees very well with experiment for penetrations of a few thousand angstroms for elements with atomic numbers of 15 and below; agreement with experiment is not as good for elements of much higher atomic number. Some other theory or an approximation of this theory should be used for penetrations of more than a few thousand angstroms, e.g., Bohr's theory. Vavilov's theory relies on Bethe's formula for average energy loss. The algorithm in YMAT avoids this dependence, and, instead, is based upon measured average energy losses.

There are many theories relating to energy loss and energy-loss straggling; however, there are few measurements available to test straggling theories. These measurements are difficult and are badly needed for work of the kind described in this report.

B. Computers and Peripheral Apparatus. Keyboard terminals located in the space of the user provide a significant advantage over the batch-processing mode at a centrally located computer for calculations of the kind discussed in this report. Keyboard-printer terminals can be augmented with video terminals, plotters, and line printers dedicated to a particular set of problems thus further reducing travel and waiting times associated with batch-processing modes at a central computational facility.

A further step in the decentralization of facilities which can increase the speed and/or ease of analyses is to provide the user with a small computer with appropriate peripherals dedicated to a particular set of problems. That support for such arrangements is prevalent can be inferred from the many specialized computers dispersed throughout some scientific laboratories. Of course, many of these units are used for on-line operations but they can also be used to great advantage for computational purposes, especially in conjunction with a large, fast machine with large disk storage capacity.

This mode of computation has been abetted significantly in the last decade by the rapid development of small computers, peripherals convenient for the non-specialist, increased equipment reliability, and falling costs. A large segment of the computer industry is devoted to rapidly improving this area.

More specifically, for data analyses of the kind discussed in this report, a suitable system might consist of a microprocessor-based computer, a floppy or hard-disk driver system, a dot-matrix impact printer (with graphics capability), a video terminal, and a link to a large, fast computer. A reasonably satisfactory system could be obtained at a cost in the neighborhood of ten thousand 1981 dollars. This cost and associated maintenance costs are small compared to probable manpower costs -- especially those needed for the generation of software.

C. Computer Languages. One useful feature of the decentralized, dedicated computer is that it can be made available to one user at a time. This permits the use of an interactive language such as Forth (6).

While present versions of Forth are not highly suited to involved numerical analysis, a few remarks concerning this interactive language follow inasmuch as it seems likely that this language and/or other interactive languages will be developed in the near future in a way that will greatly increase the convenience of data analyses such as those described herein. At present, Forth is highly suited to on-line use with systems of instruments.

A Forth-language resident system occupies about 10K to 15K bytes of memory. It includes a high-level language, an assembly language, a compiler, two interpreters (text and address), a set of named (and compiled) modules, a dictionary containing the module names, their addresses, and addresses which link them to other related modules. Some versions also have text-editing and file-handling software.

The user "programs" by creating new named modules based upon names existing in the dictionary, by creating new named modules from assembly language, by creating new classes of named modules, including control structures, data structures, and other programming tools. A module is compiled at the time that it is entered into the dictionary via the keyboard and the new name can be used in the same manner as the original names. Thus, this language has enormous flexibility and extensibility; the user, in effect, creates a language suited to the problem at hand.

The names in the dictionary constitute the high-level language. The names (operators) are executed singly or in sequences immediately after entry (in inverse Polish Format) to produce computations or input/output (I/O). Thus, if one wishes to produce a long sequence of computations leading to a final set of numbers and/or graphs, an operator or operators may be executed to produce a segment of the total with intermediate diagnostic I/O -- or the entire sequence.

Computer languages of this kind are sometimes referred to as block-diagram languages with the compiled modules being the blocks. The interpreters parse the entered statements, consult the dictionary, and "point" the computer to appropriate modules. Programs utilizing this kind of software are sometimes referred to as threaded code, with the addresses in the dictionary being the thread that links the modules at execution time.

The use of a language of this kind obviates the necessity for re-compiling and linking programs when a small change is made. Changes can be made by redefining operators rather than by changing programs -- if the user prefers.

While computers are necessary for complex problems, they tend to enslave the people who interact with them. There is a need to devise better modes of interaction to reduce the tedium, enslavement, and dependence on large-system protocol. Hopefully, the foregoing remarks can be of help in this area of endeavor. We may look forward to more powerful computers and peripheral units at prices that permit interactive computing. It also seems likely that eventually large libraries of modules for interactive languages will be developed, stored on floppy disks, transmitted from one computer memory to another, and distributed commercially at reasonable prices.

VII. ACKNOWLEDGMENTS

Many of the measurements upon which this report is based were made in collaboration with Mr. H. L. Hughes who has made so many contributions to the radiation hardening of solid-state electronic devices and with Dr. P. R. Malmberg and Mr. C. A. Kennedy who have made so many indispensable contributions to the NRL Van de Graaff accelerator and ancillary apparatus. Essential also to the work upon which the report is based are the contributions to nuclear physics and some very sophisticated instrumental developments made by Drs. R. O. Bondelid and J. W. Butler. Finally, acknowledgement of encouragement, advice and support over many years is extended to Drs. J. McElhinney and E. A. Wolicki.

REFERENCES

1. K. L. Dunning and H. L. Hughes, IEEE Transactions on Nuclear Science, NS-19, No. 6, 243 (1972)
2. R. O. Bondelid and C. A. Kennedy, "A Two-meter Positive-ion Electrostatic Analyzer", NRL Report 5083 (1958)
3. P. V. Vavilov, Zh. Eksp. Teor. Fiz. 32, 320 (1957)
4. R. D. Evans, "The Atomic Nucleus", McGraw-Hill Book Co. Inc., New York, N. Y. (1955) p. 661
5. S. M. Seltzer and M. J. Berger, Nuclear Science Series Report 39, National Academy of Science Series - National Research Council, Washington, D. C. (1964) p. 187
6. The journal BYTE, 8, Aug., 1980 contains several introductory articles concerned with the Forth language.

APPENDIX

NRL ASC7 COMPUTER CATALOG STATUS TABLE FOR NODE USERCAT/D66/B00/DUNMK1/NRP

SCNS: (as of 1 August, 1980)

HLP1	HLP3	HLP4	HLP5	HLP7	HLP8
SL1DATA5	OL1DATA5	LM1DATA5	IX2HHOS5	OX1HHOS5	SL8YMULT
OL8YMULT	LM8YMULT	SL9YMAT	OL9YMAT	LM9YMAT	IMHHOS5
IN2TGT7	MA2TGT7				